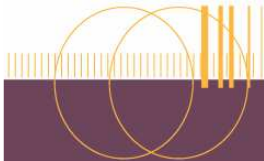


Mechanical Properties of ultrafine-grained Iron processed by HIP

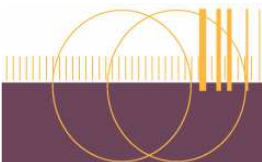
G. DIRRAS

LPMTM-CNRS, UPR 9001
Institut Galilée, Université Paris 13
99, avenue JB Clément
93430 Villetaneuse

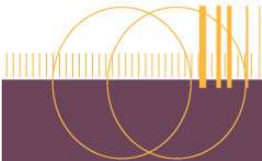


- ¹Standard polycrystals vs nanograined polycrystals: what do we know, what do we measure?

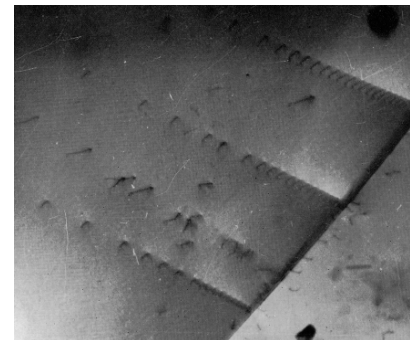
¹ Collaboration: G. Saada. LEM, ONERA, Châtillon



- The general principles underlying the processing of high strength, and ductile, metallic materials have been understood since the beginning of the development of dislocation theory.
- Ductility necessitates a reasonable mobility of the dislocations, strengthening is related to the building of obstacles restricting propagation of dislocations.

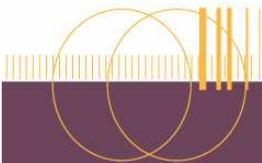


- These obstacles (dislocations, atoms in solid solution, second phase inclusions, grain boundaries) are introduced by combining alloying (structural hardening), plastic flow (strain hardening) and **grain size refinement**.

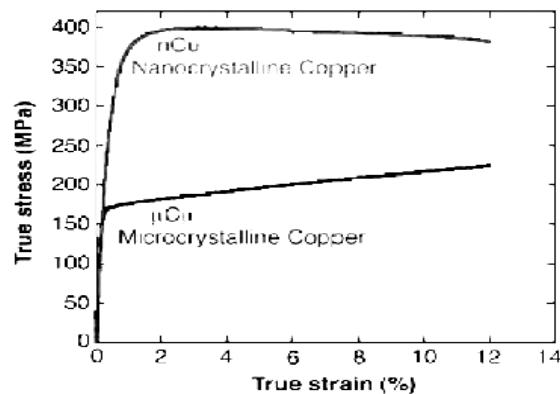


Dash et al. (1956)

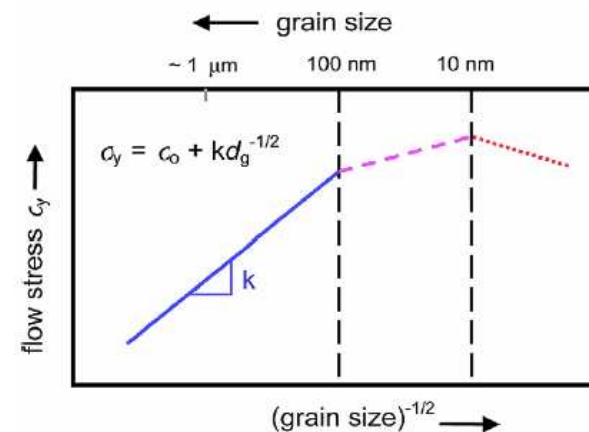
Hall – Petch Law:
$$\sigma = \sigma_0 + \frac{k}{\sqrt{d}}$$



- Down to very small grained materials, one expects an increase in strength, which has been observed in various circumstances .



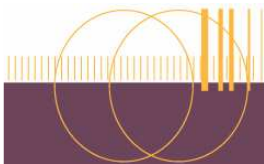
(Champion et al. Science **300**, 310 (2003))



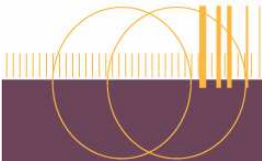
Kumar et al. Acta Mater., 51 (2003) 5743-5774)

Various mechanical tests on these products have revealed indeed a remarkable increase of strength, at the expense of ductility. But the measured values of the yield stress significantly differ from those obtained by extrapolating the HPL formula

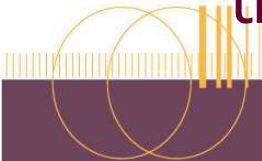
$$\sigma = \sigma_0 + \frac{k}{\sqrt{d}}$$



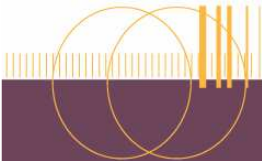
- This has stimulated the processing of polycrystals of smaller and smaller grain size, which have been classified, with respect to their grain size, as:
 - *microcrystalline (mc)* if $d > 1000\text{nm}$,
 - *ultra fine crystalline (ufc)* if $100\text{nm} < d < 1000\text{nm}$,
 - and *nanocrystalline (nc)* if $d < 100\text{nm}$
- Processing methods include: powder compaction, electro-deposition, SPD...



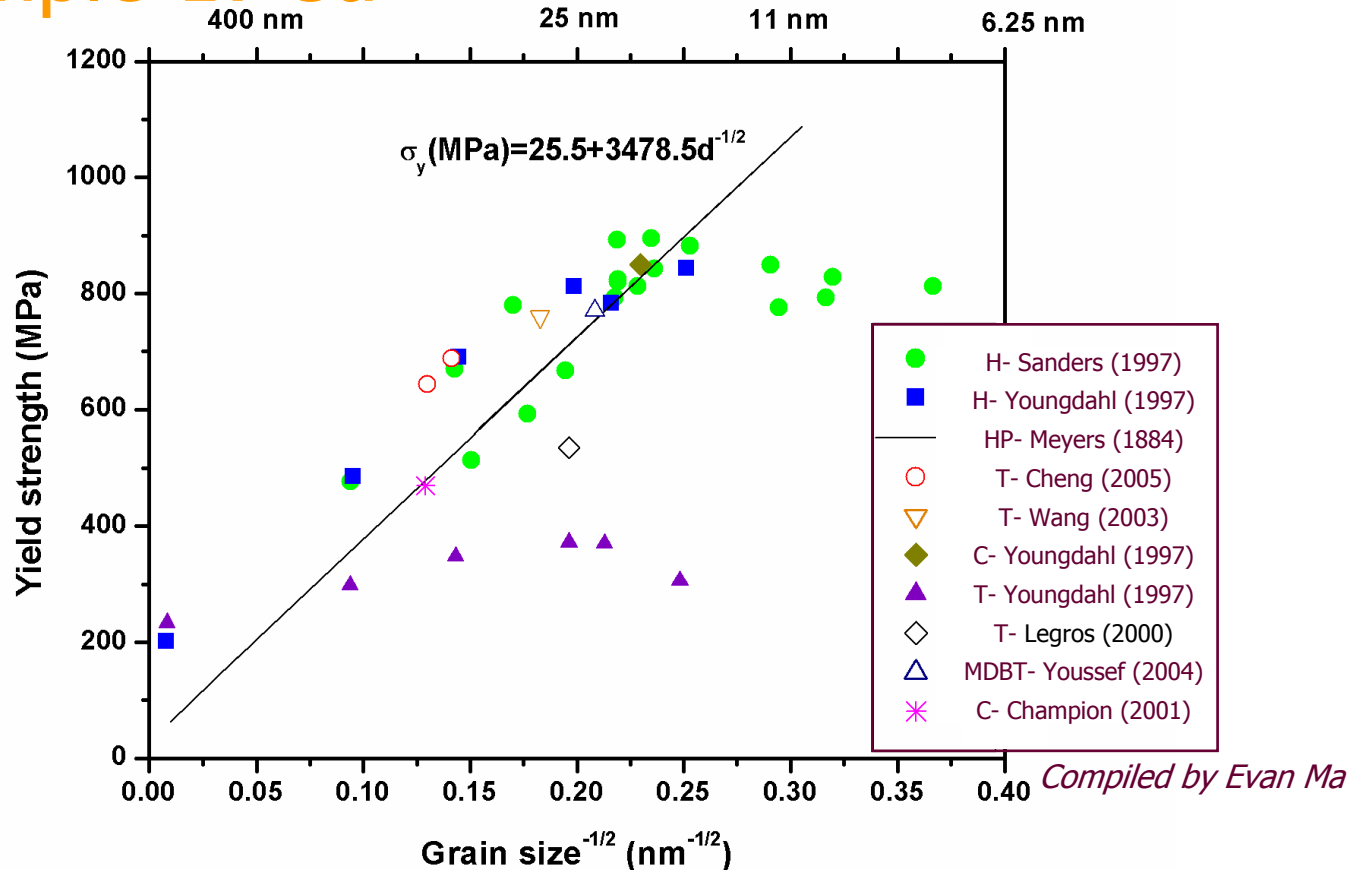
- Our present understanding of the deformation mechanisms of standard polycrystals depends on:
 - the production of specimens with well designed and characterized microstructures.
 - the gathering of consistent and systematic data through mechanical tests over a wide range of strain rates and in a large temperature interval.
 - A thorough observation of the evolution of the microstructure during mechanical testing.
 - Establishing a consistent correlation of the mechanical behavior with the microstructure by a relevant theoretical analysis.



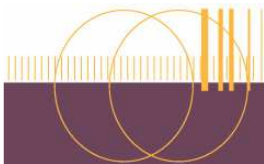
- As far as nano grained polycrystals are concerned, today's situation is characterized by:
 - *Limited control and description of the as prepared microstructure*
 - *Incomplete information on the evolution of the microstructure*
 - *Inaccuracy of the measurement of the relevant mechanical parameters*
 - *Inadequate theoretical interpretation*



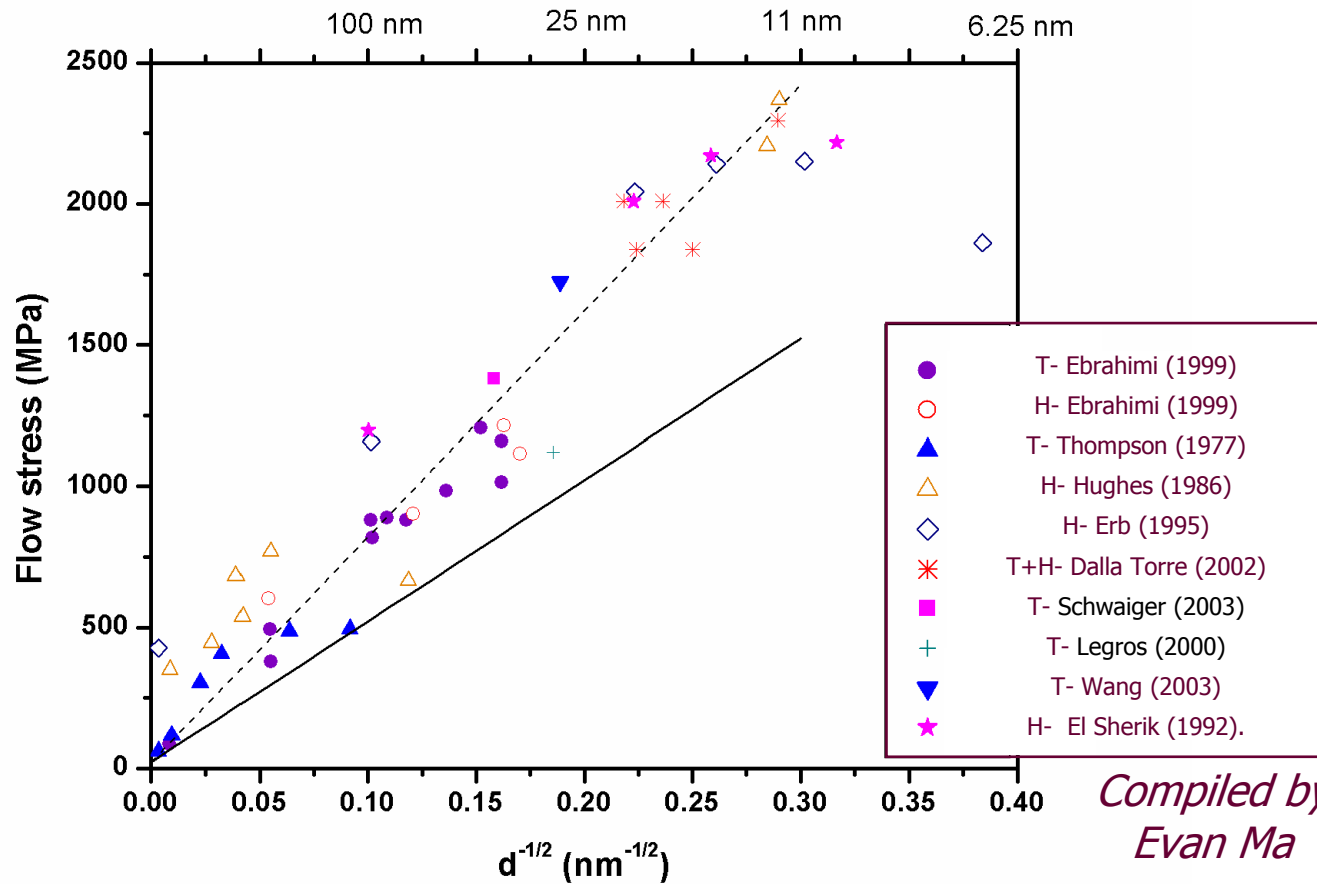
Example 1: Cu



In the case of *sp*, there is a general, and justified agreement on the relevance of the identification of the 0.2% proof strain flow stress $\sigma_{0.2}$ to the yield stress σ_y , as well as the latter to a fraction, generally 1/3, of the Vickers hardness H_V .



Example 2: Ni



Various mechanical tests on these products have revealed a remarkable increase of strength. But the measured values of the yield stress significantly differ from those obtained by extrapolating the HPL formula



Example 3

The smallness of the grain size of *ngp* imposes very strong constraints. This imposes to revisit the meaning of concepts such as elastic-plastic transition, macroscopic and microscopic yield stress,...

$$\varepsilon_M > \frac{b}{d}$$

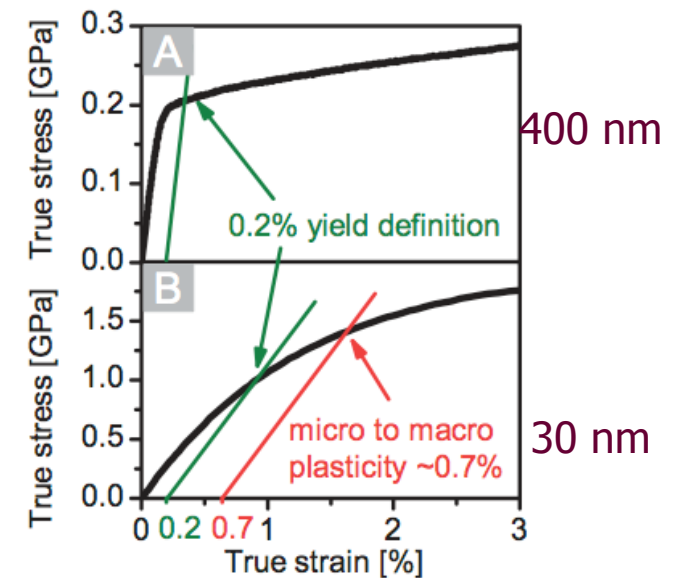
At $\varepsilon_M = 0.2\%$ $\rightarrow d > 500b \approx 125\text{nm}$
($b \approx 0.25\text{nm}$)

Moreover at 0.2% strain, the fraction of deforming grains is:

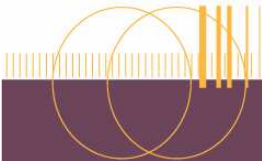
$$\frac{n(\varepsilon_M)}{N} \approx \varepsilon_M \frac{d}{b} = 2 \times 10^{-3} \frac{d}{b}$$

$$d \leq 20b \Rightarrow \frac{n}{N} \approx 4\%$$

Saada, Mater. Sci. Eng., 400 (2005) 146-149



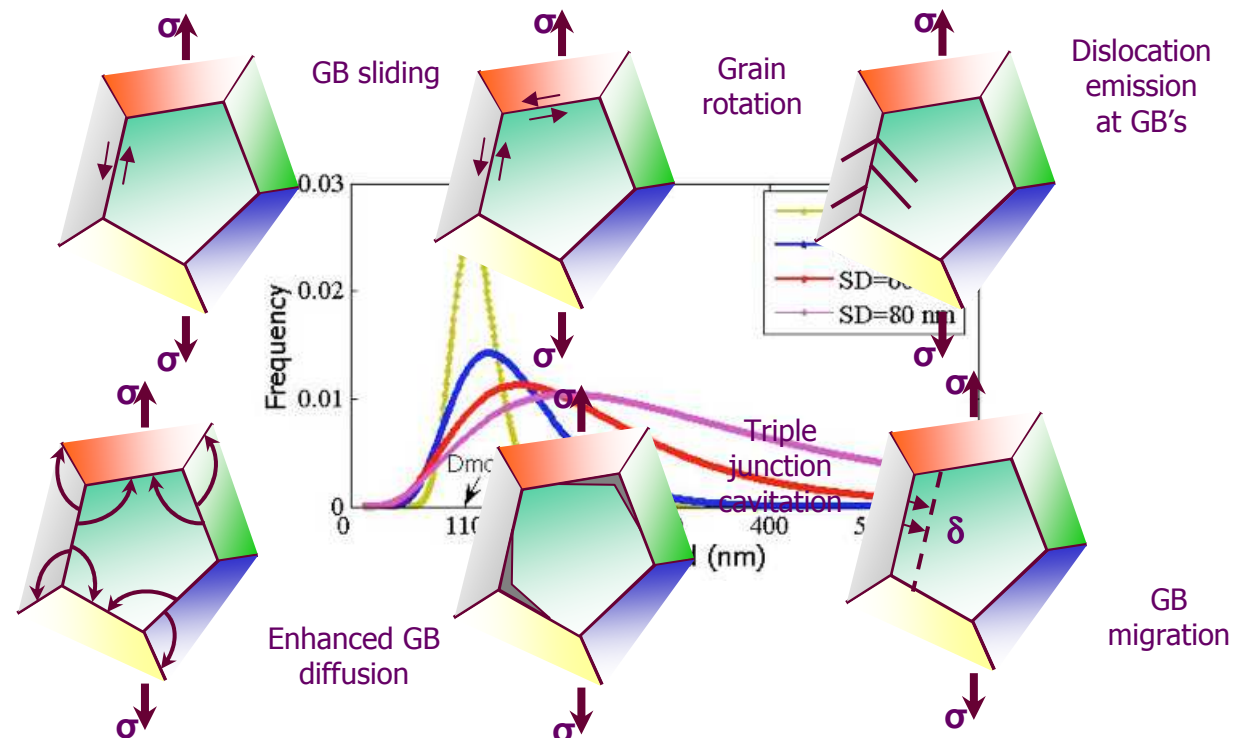
Brandstetter et al. Adv. Mater., 16
(2006), 1545-1548



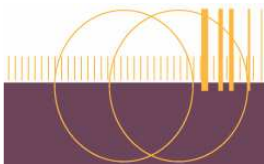
Example 4: deformation mechanisms

- Samples usually exhibit a Log normal grain sizes distribution
- The observed mechanical behavior is a complex interplay of different processes

Proposed nc-deformation mechanisms

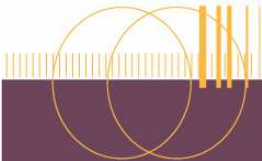


D. Gianola, T. Rupert, K. Hemker "Experiments in grain boundary dominated materials". Braunwald, Switzerland, September 2007.



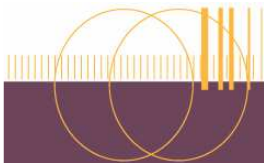
Since the grain size alone neither defines the microstructure nor characterizes the mechanical behavior of these very small-grained polycrystals, we shall distinguish simply:

- *micro-grained polycrystals (mc)* whose grain size is larger than one or a few microns,
- *ultrafine-grained polycrystals (ufg)* whose grain size is smaller than one micron

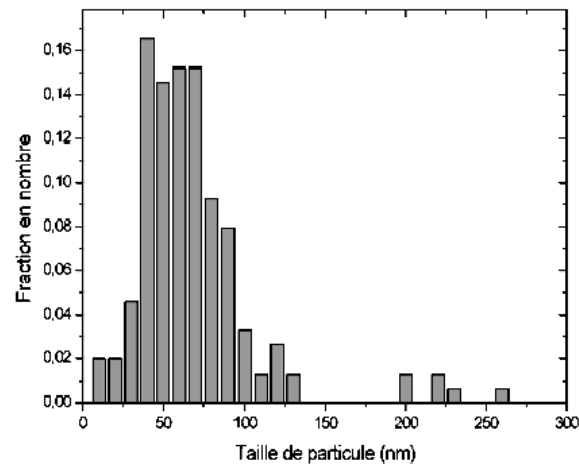
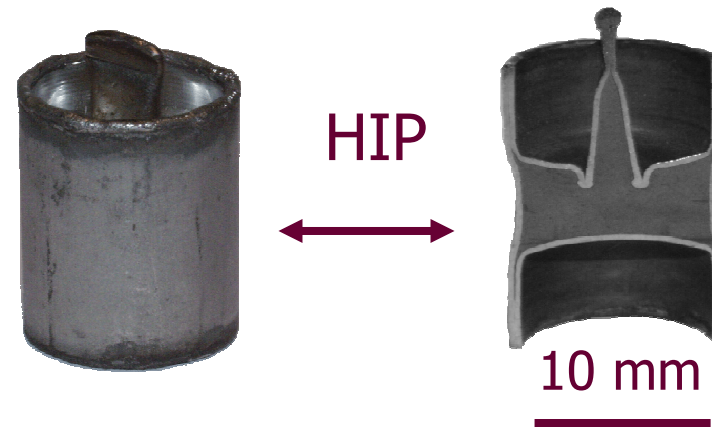
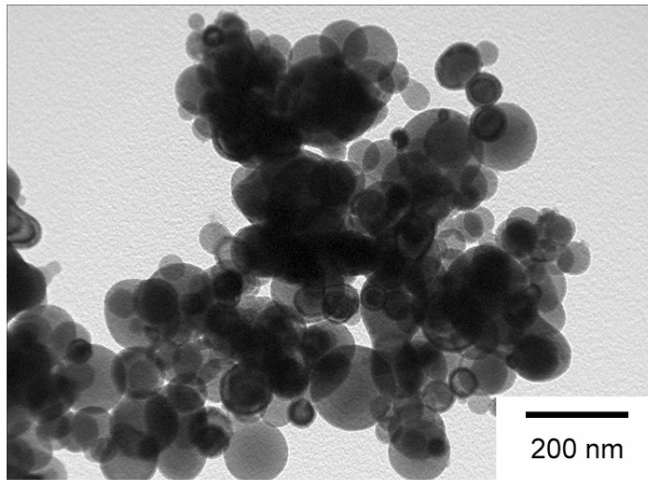


- *HIP processing of ultrafine grained Iron: Mechanical properties

* RNMP AGUF (with ARCELOR)

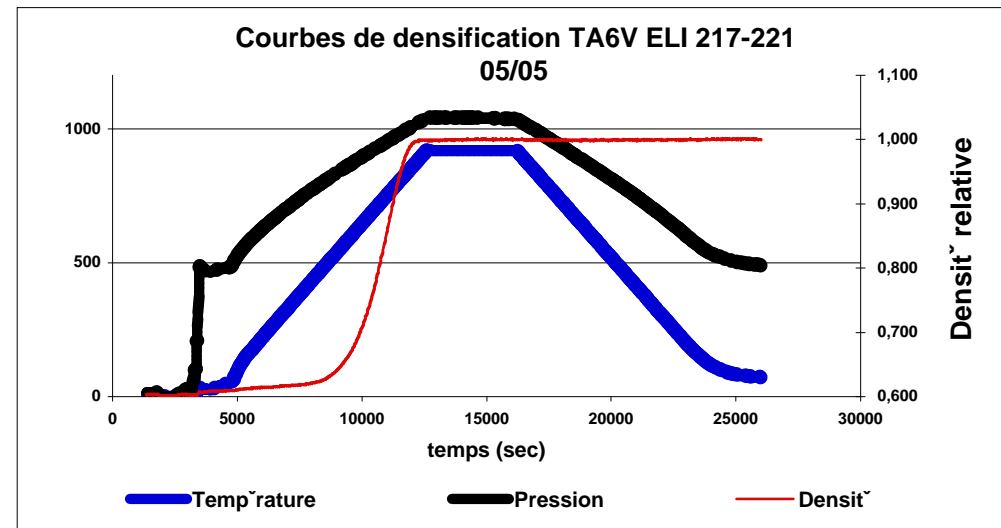


Starting materials and the HIP process

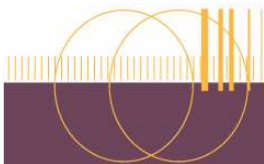


Commercial purity Iron powders
Obtained by EEW from *Argonide Corp., USA*

Fe, Fe₃O₄...



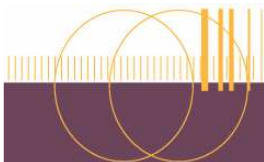
Stainless container
Pressure applied through *Ar* gas



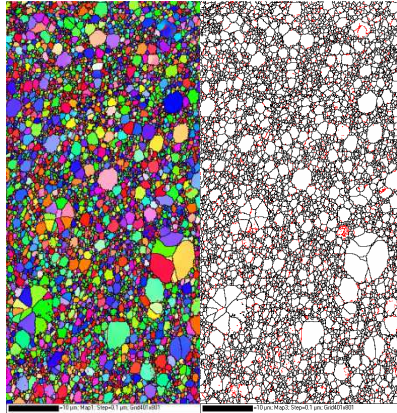
Optimized HIP parameters for the Fe powder

Oxide reduction at 450°C	Sample ID	Fe200	Fe201	Fe203	Fe205
	Time (h)	3	3+4*0.5	6*0.5	8*0.5
	# steps	-	4	6	8
HIP	Holding Press. (MPa)	120	110	155	200
	Holding T° (°C)	800	800	720	620
	Holding Time (h)	2.5	14	1.5	2.5

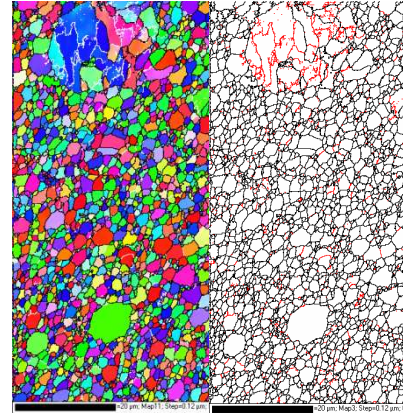
Compact density > 99



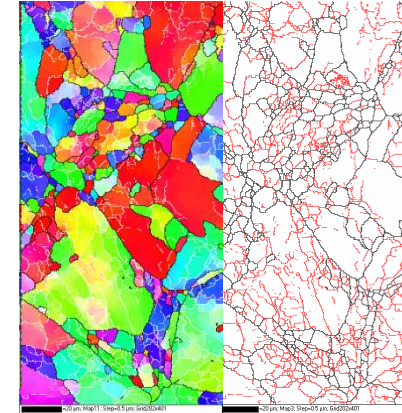
As-processed microstructures



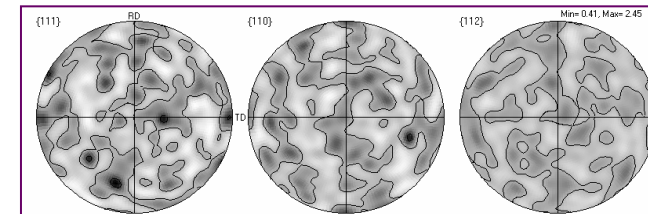
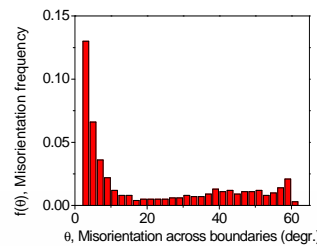
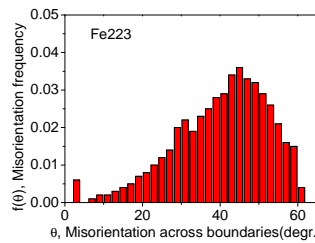
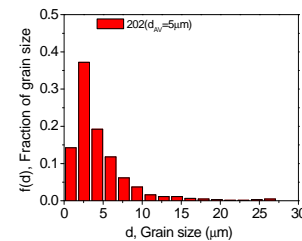
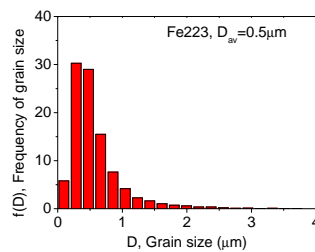
0.5 μm



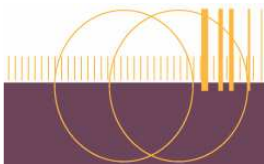
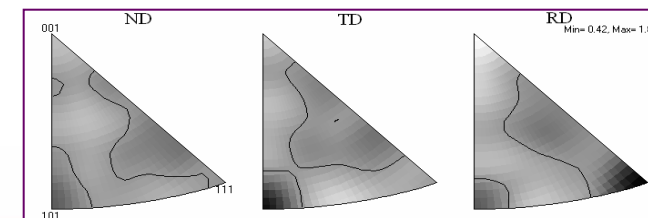
1.0 μm



5.0 μm



Random initial crystallographic texture



Mechanical behavior

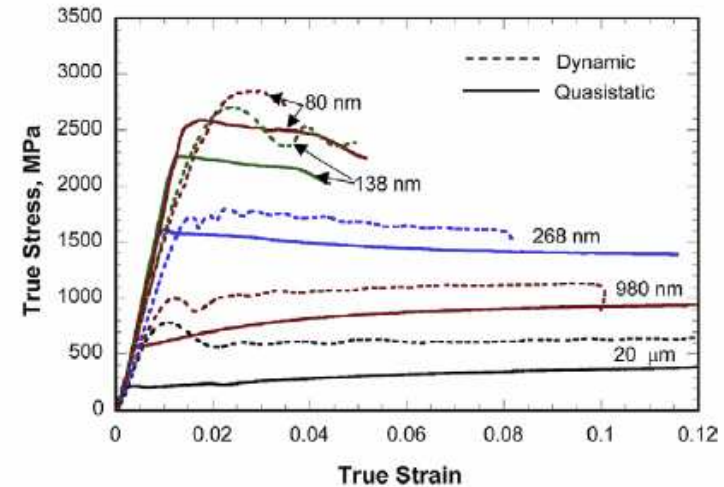
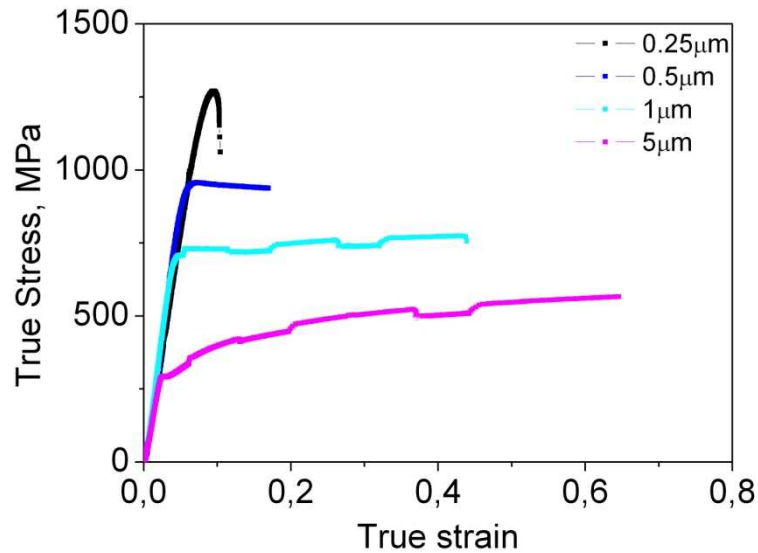
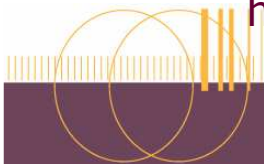


Fig. 2. Typical stress-strain curves obtained for the consolidated iron under quasistatic ($1-4 \times 10^{-4} \text{ s}^{-1}$) and high-strain-rate ($3-6 \times 10^{+3} \text{ s}^{-1}$) uniaxial compression for all of the grain sizes.

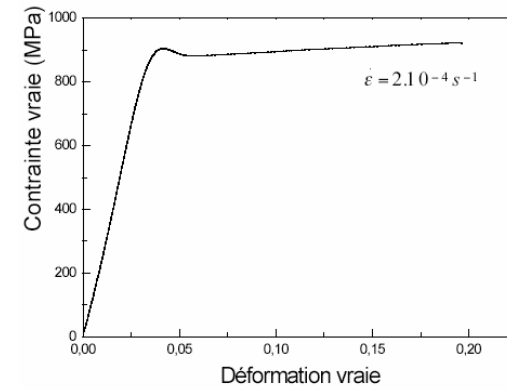
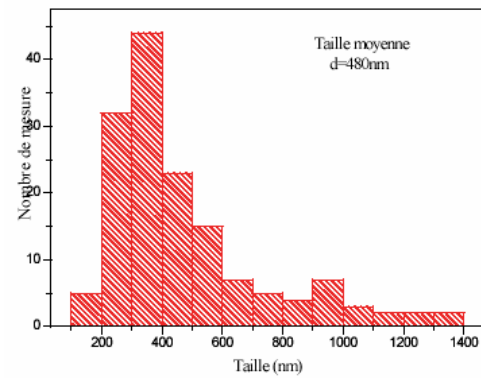
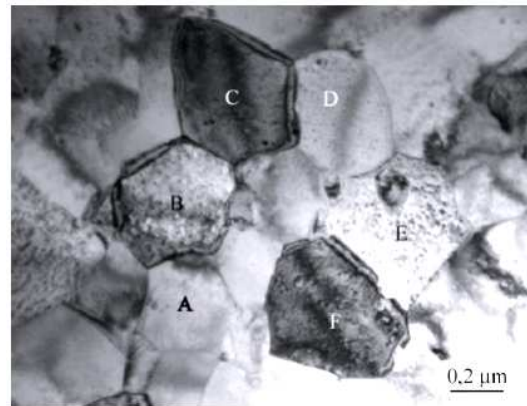
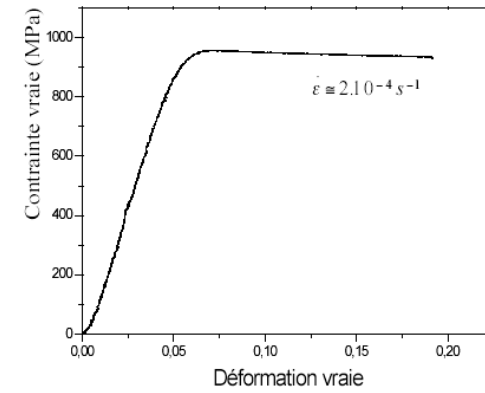
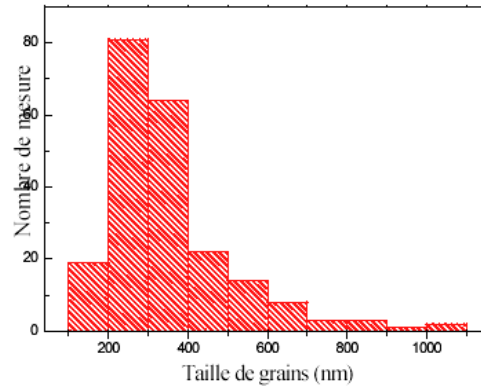
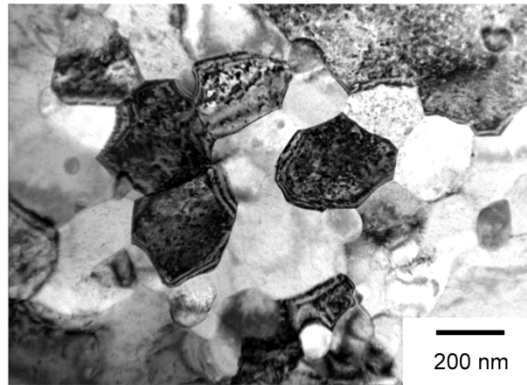
Quasistatic compression test at RT:

- Increase in strength
- Transition of the deformation mode from hardening to softening

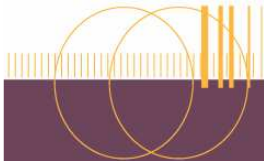
D. Jia et al. Acta Mater. 51 (2003) 3495



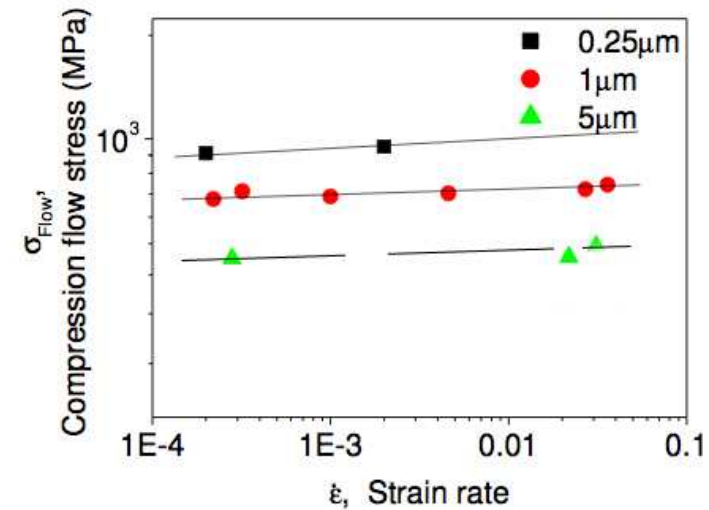
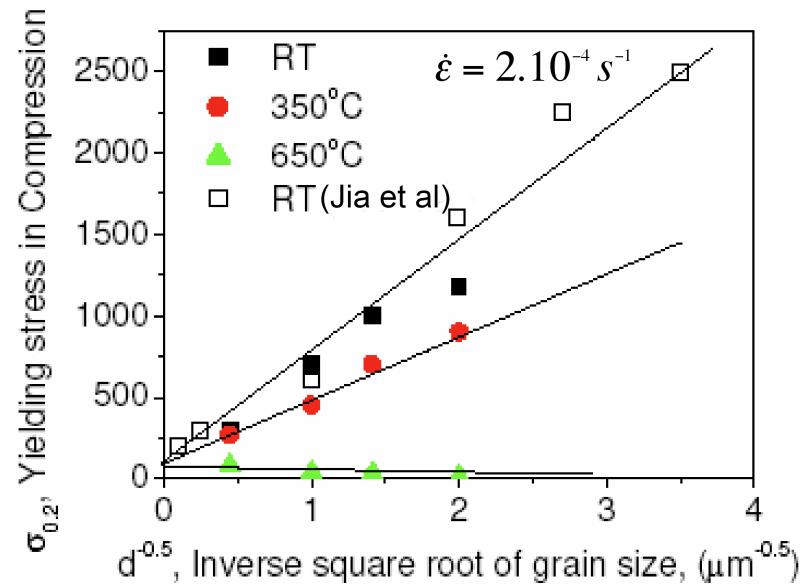
Note: this behavior depends also on the grain size distribution



Grain size distribution effect

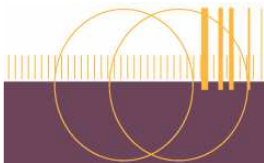


Evolution of the mechanical properties

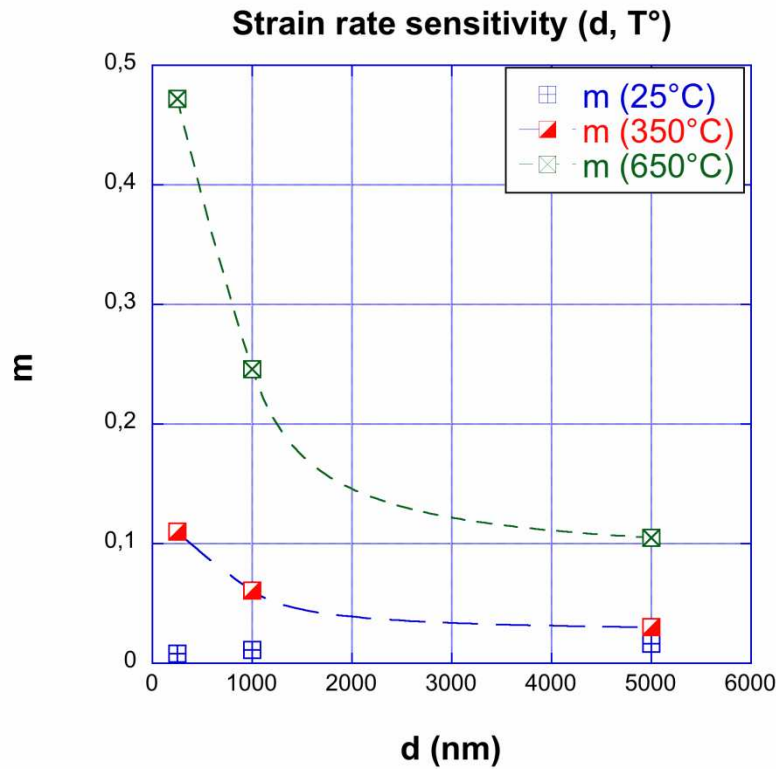


Low strain rate effect on the flow stress in the range $10^{-4} \sim 10^{-1} \text{ s}^{-1}$ at RT

$$\sigma = \sigma_0 + \frac{K_{H-P}}{\sqrt{d}}$$



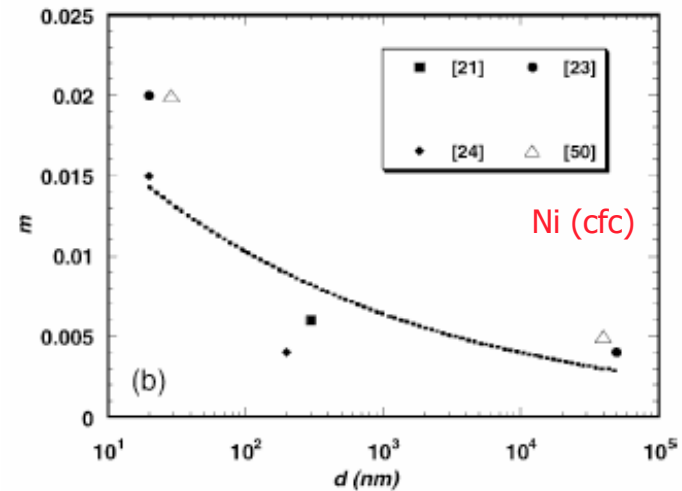
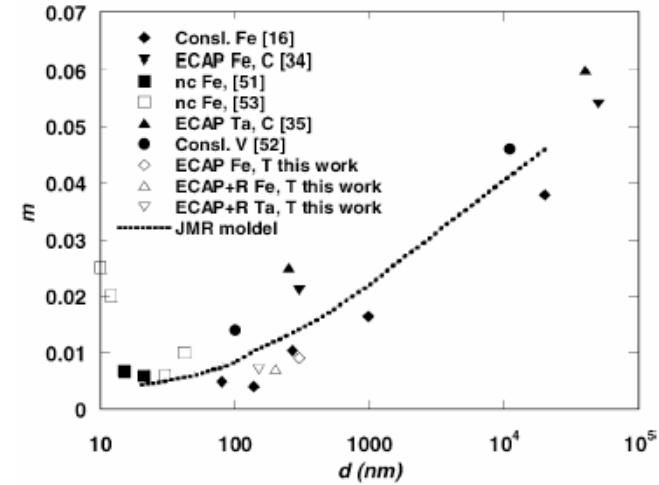
Strain rate sensitivity dependence on d and T



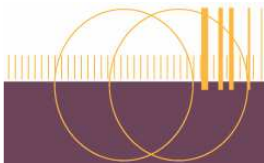
Activation volume at RT

$$V_{\text{ufg}}^*: 20-50b^3$$

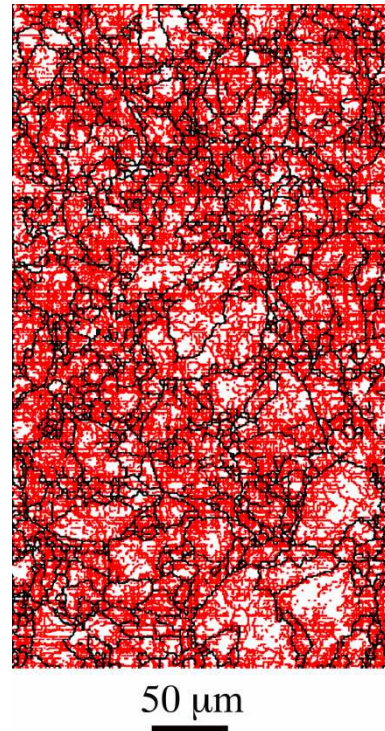
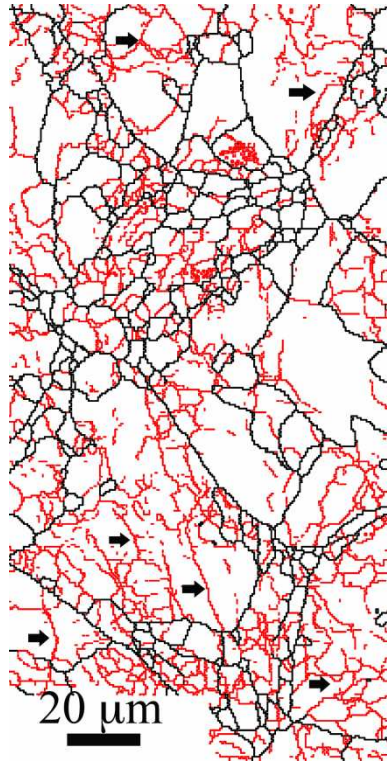
$$V_{\text{conv.}}^* \approx 10b^3$$



Wei et al., Mat. Sci. and Eng. A (2004)

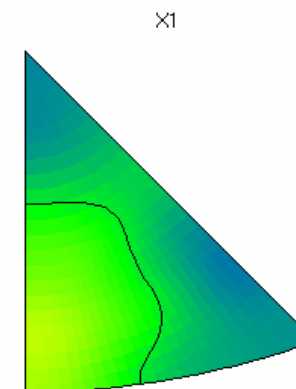
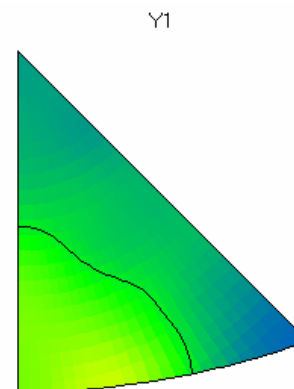
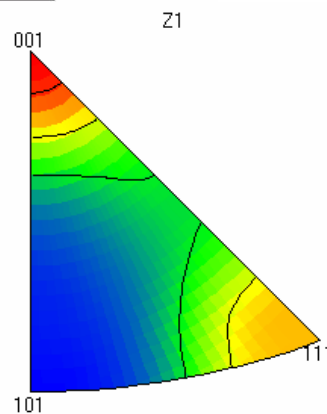
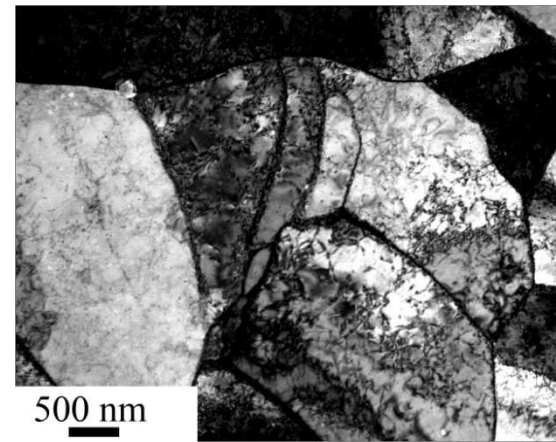


Microstructure evolution: mc iron, RT

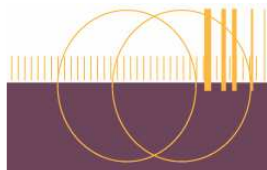


High density of SAGBs

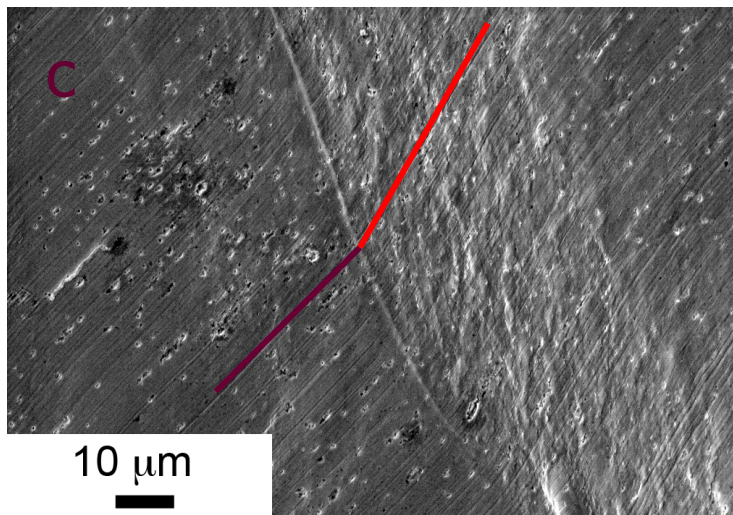
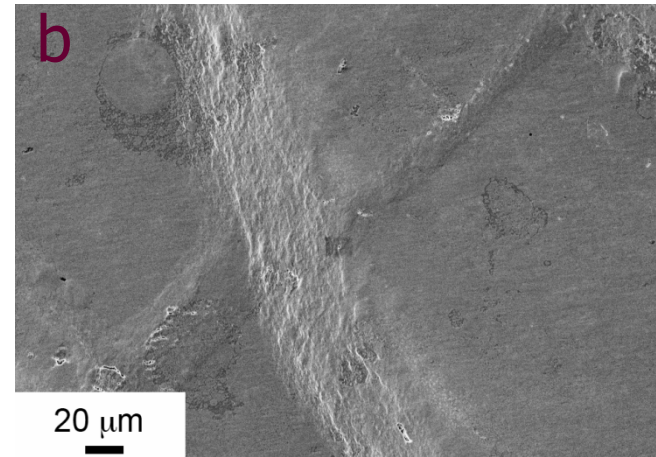
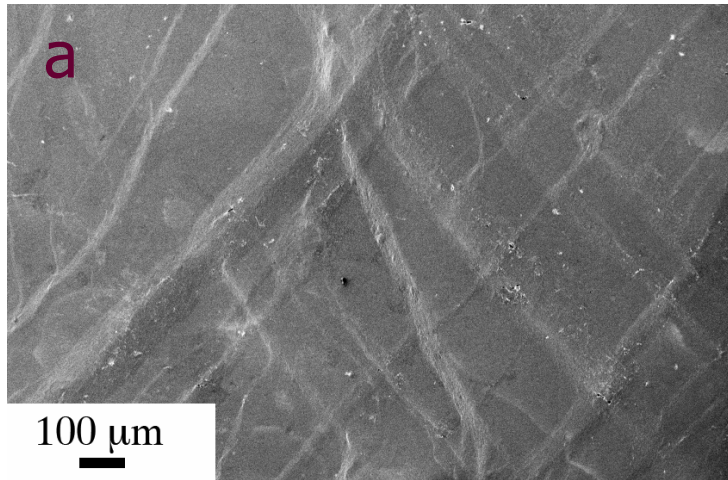
Two texture fibers // compression axis (ND)



Inverse Pole Figures (Folded)	
[202rt2-Subset1.cpr]	
Iron (Alpha) (m3m)	
Complete data set	
37143 data points	
Equal Area projection	
Upper hemispheres	
Half width: 10°	
Cluster size: 5°	
Exp. densities (mud):	
Min= 0.08, Max= 3.14	
1	—
2	—
3	—
	1
	2



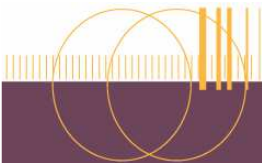
Microstructure evolution: ufg iron, RT



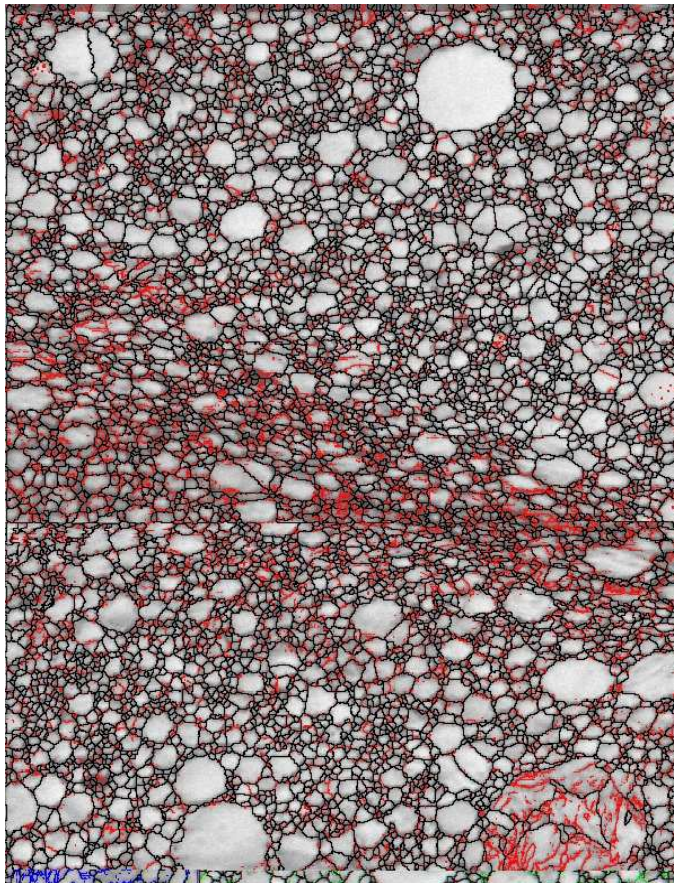
Deformation localizes within
shear bands (a, b, c)
Deformation is compatible (a)
Intense shear (c)

$\epsilon = 15\%$; RT;

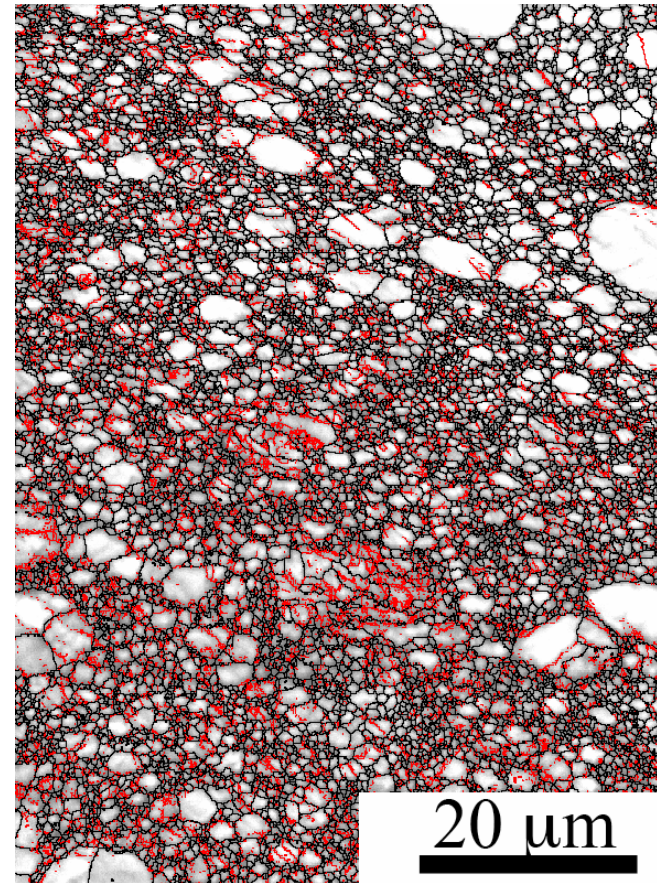
Grain size = 0.5 μm



EBSD analysis (*ufg* materials, RT)

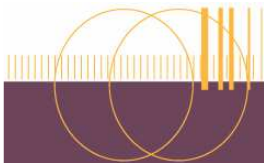


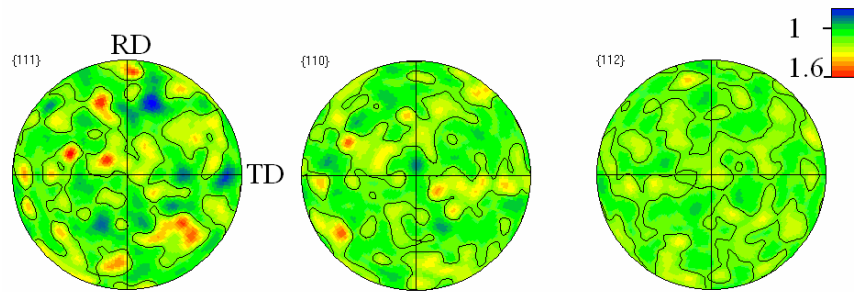
single SB



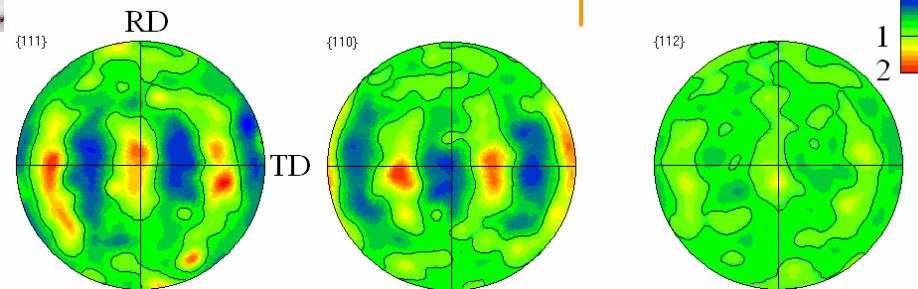
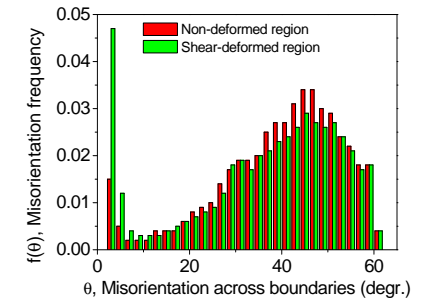
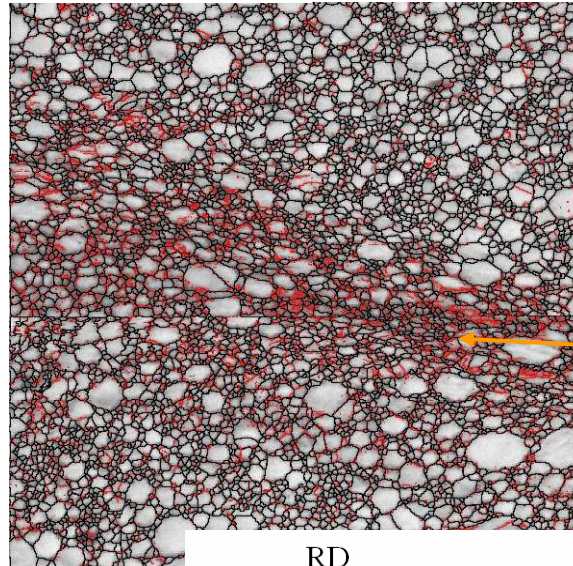
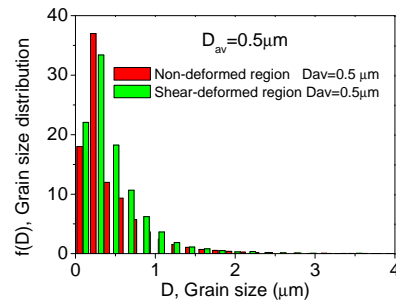
wide SB

High density of SAGBs within de SB: the deformation apparently by motion of lattice dislocations



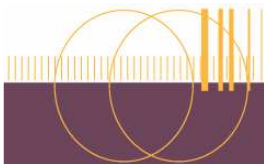


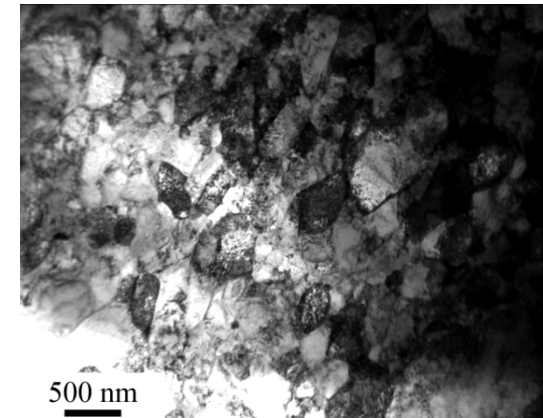
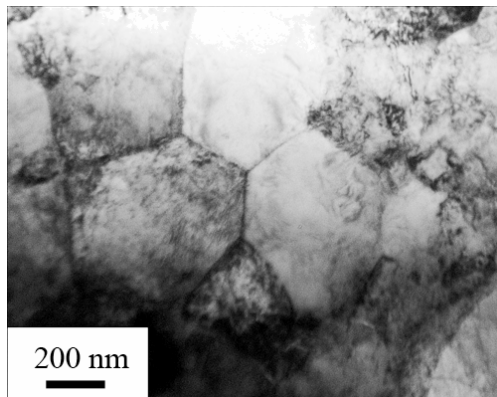
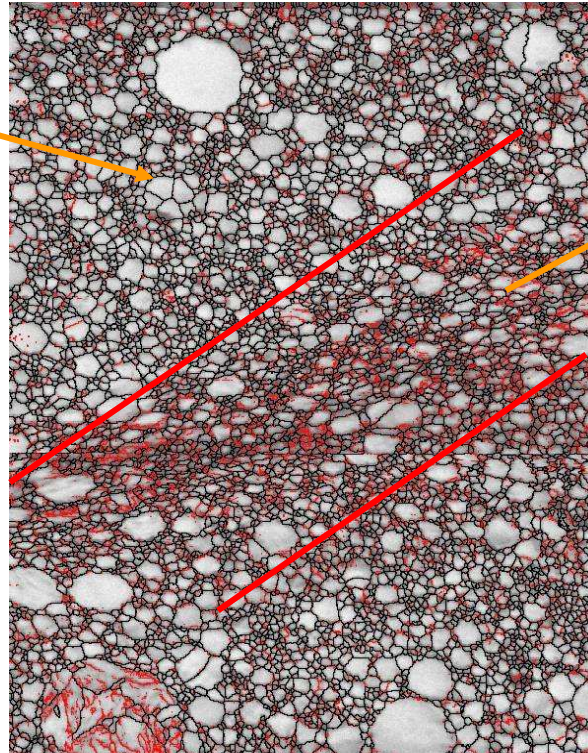
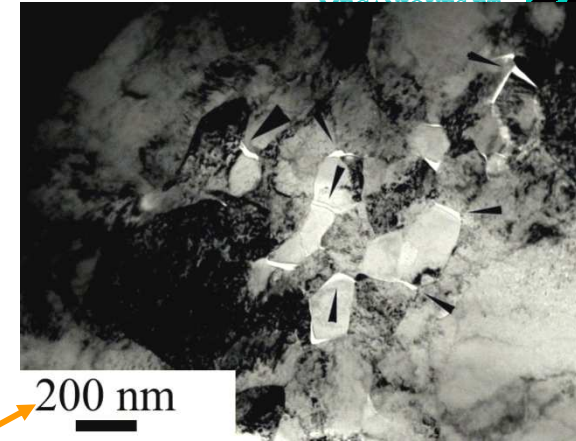
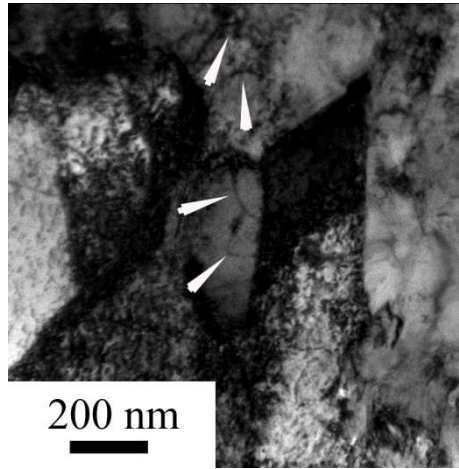
(a)



(b)

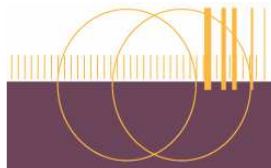
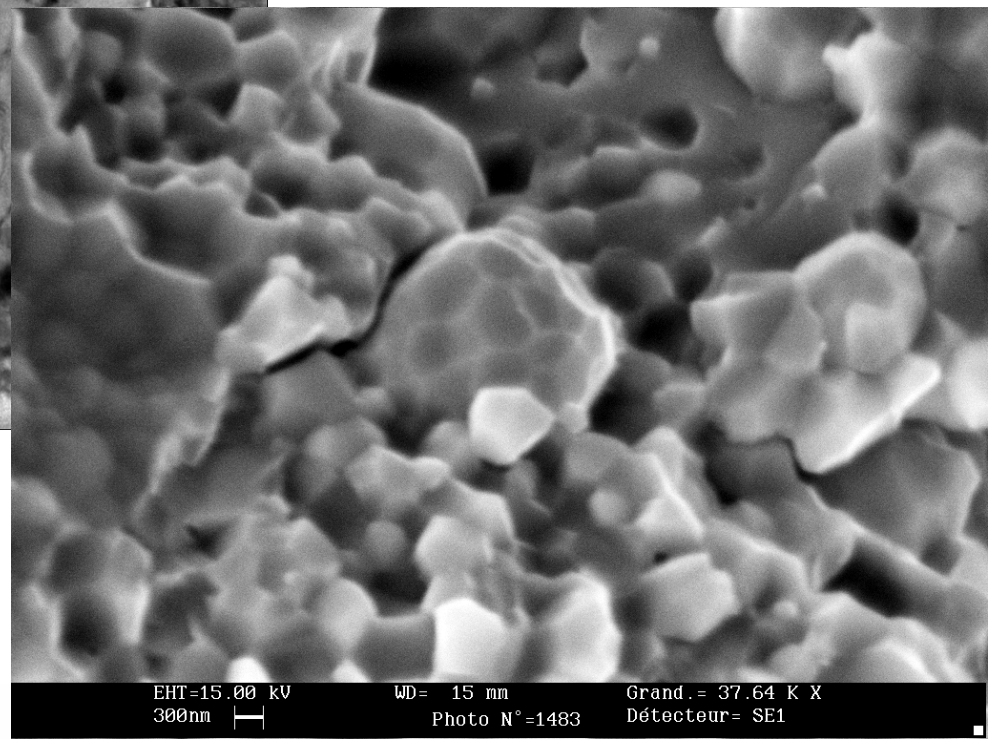
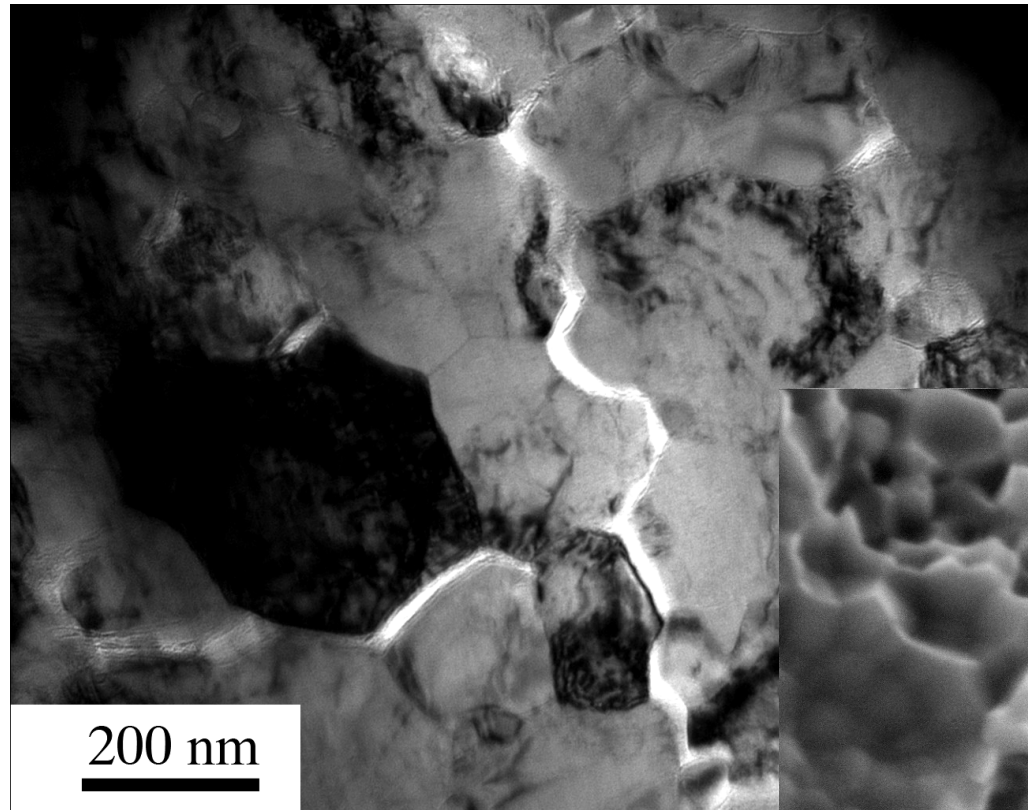
Heterogeneous deformation mode. (a): random texture outside the SB; (b) building of a [111] texture inside the SB region.



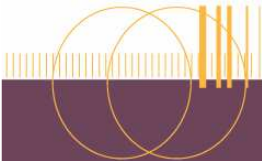


Details of the microstructure by combined TEM + EBSD experiments

Inter granular fracture mode (at RT)

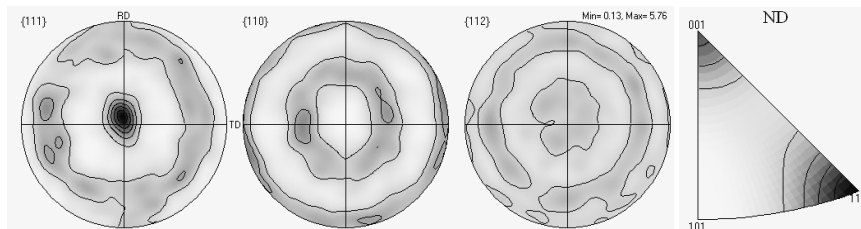
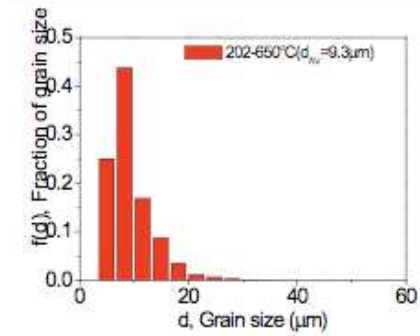
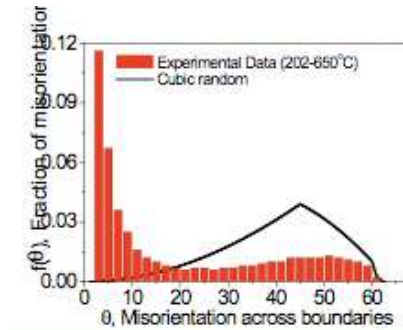
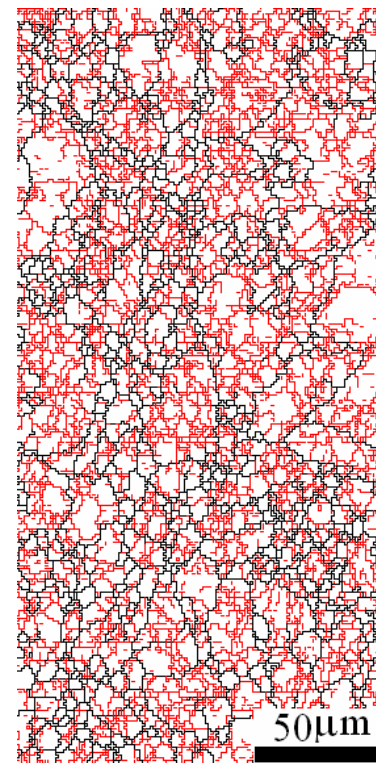
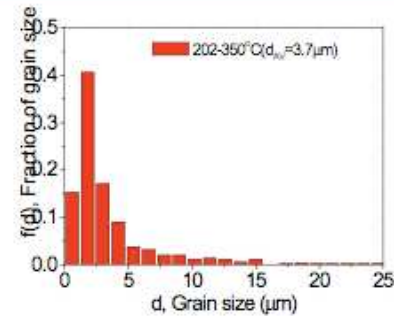
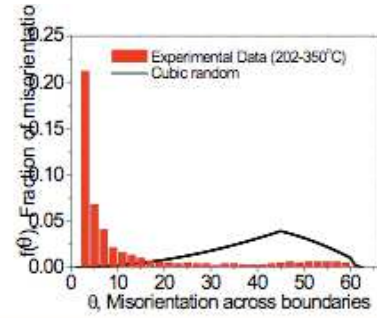
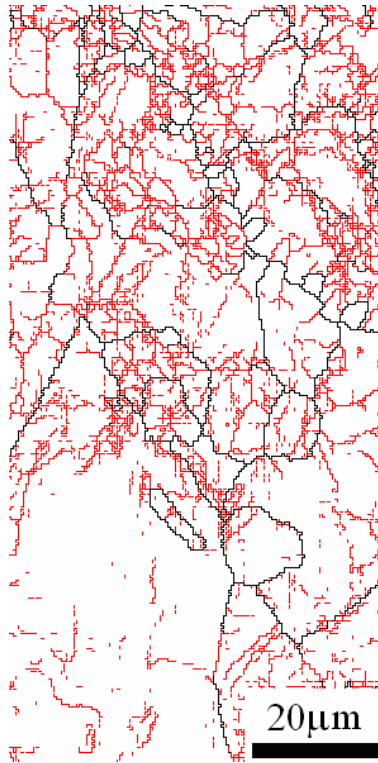


- Temperature effect on the microstructure

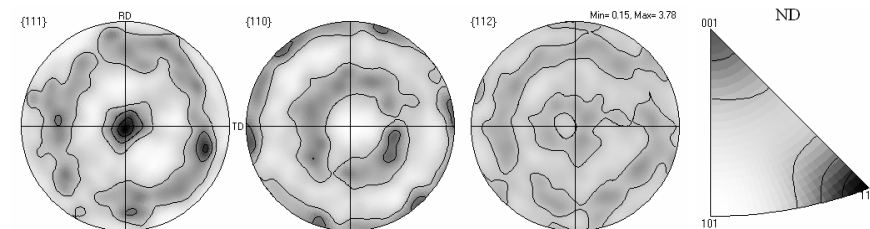


350°C

mc materials



High density of SAGBs

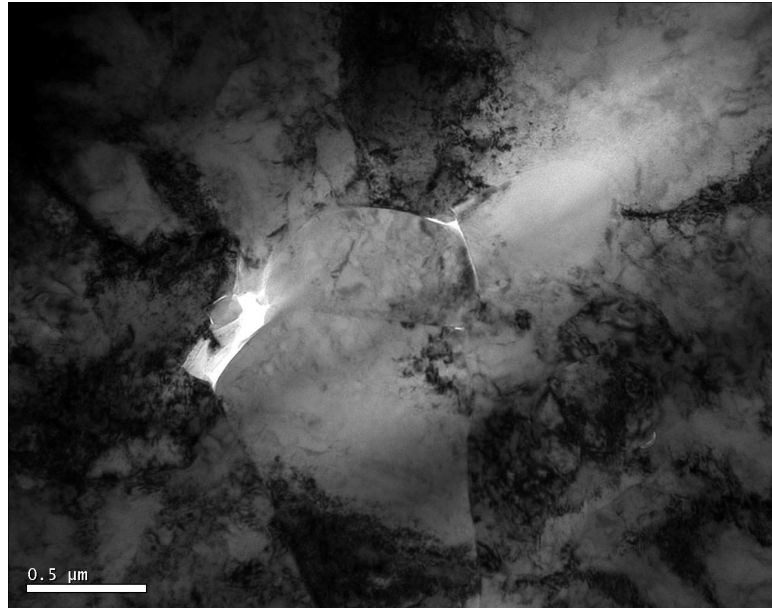


Two Strong texture fibers

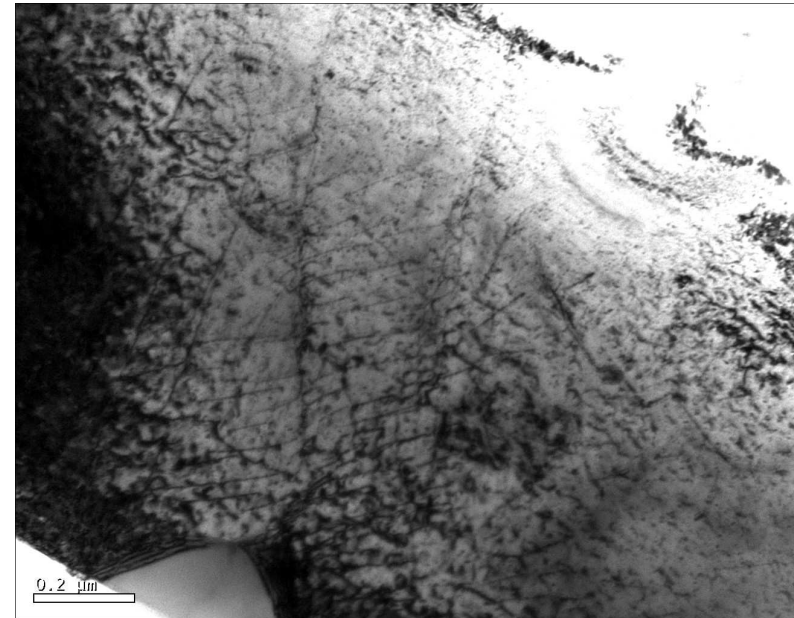
No shear banding

mc materials: TEM

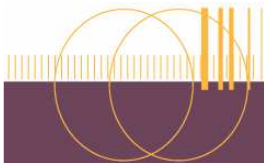
350°C



650°C

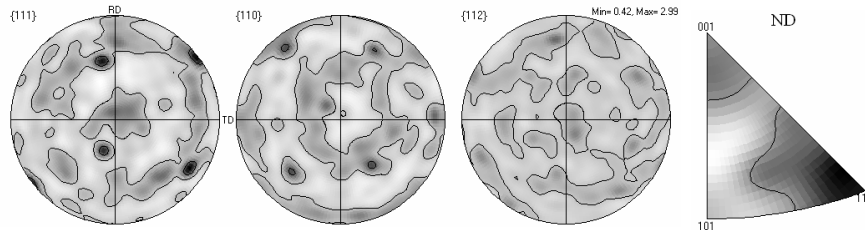
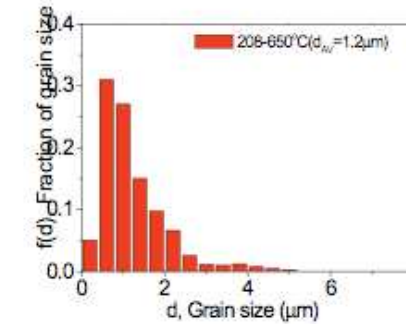
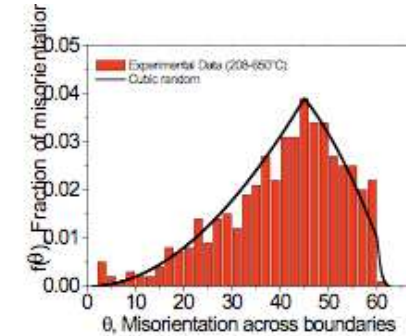
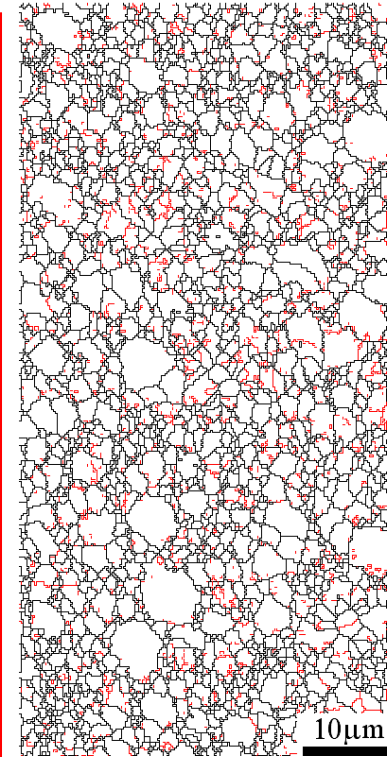
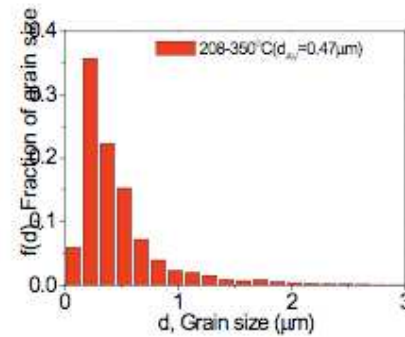
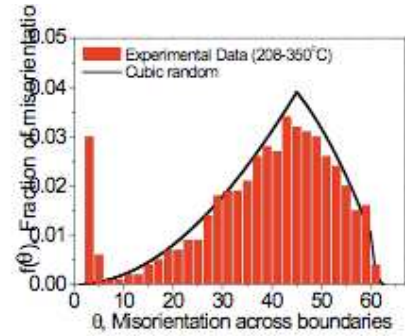
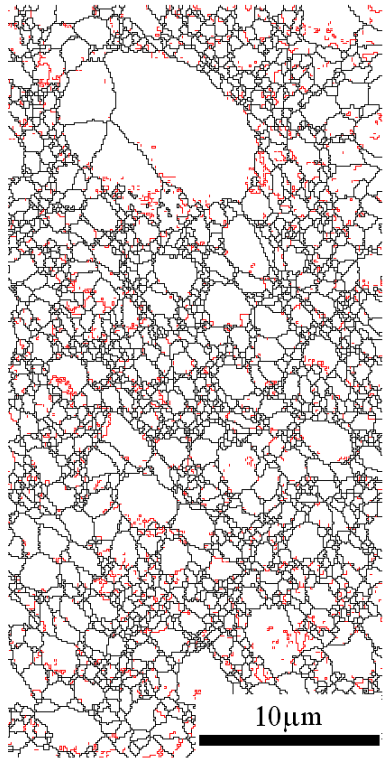


Plastic deformation by lattice dislocations, triple junction cavitation

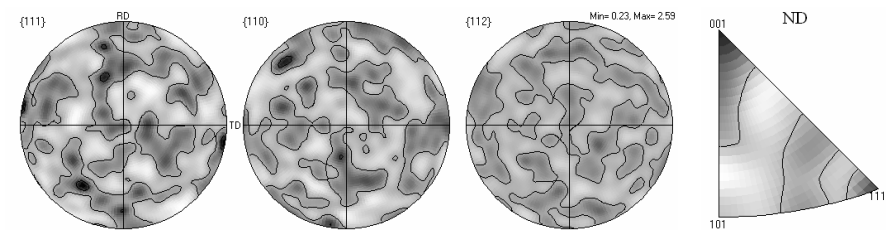


Ufg materials

350°C



weak density of SAGBs

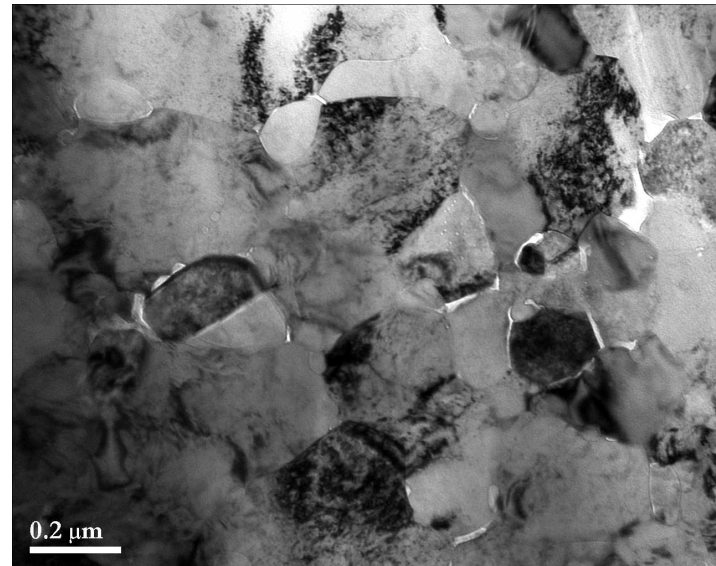


Random crystallographic texture

No shear banding

350°C

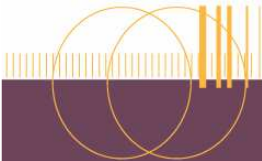
Ufg materials: TEM



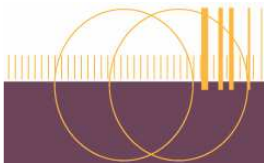
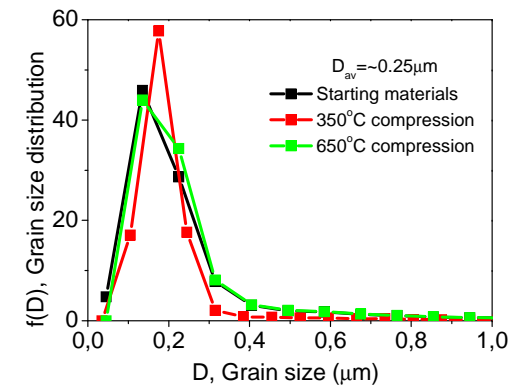
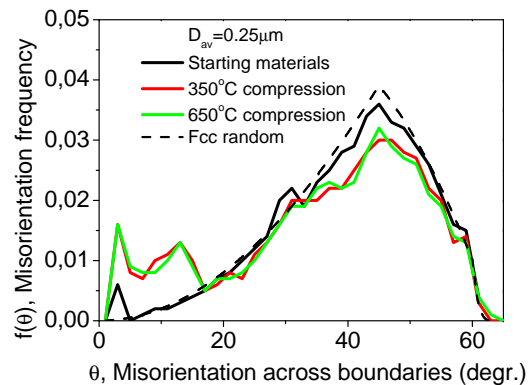
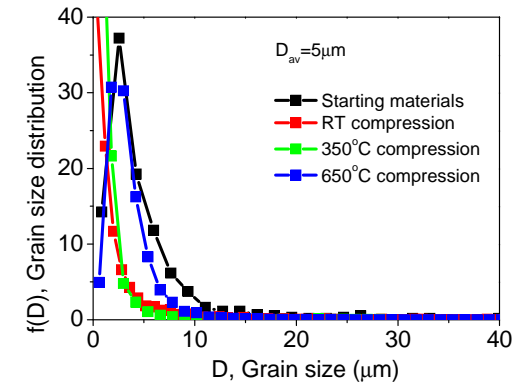
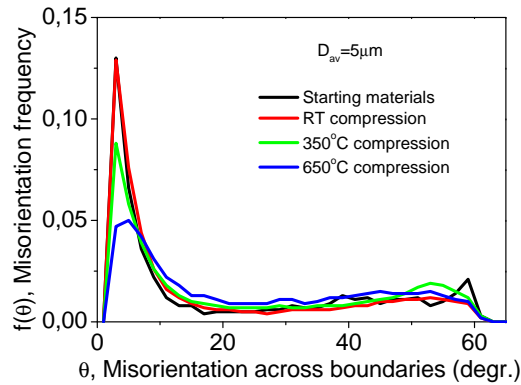
weak density of SAGBs

equiaxed grains

No shear banding



The deformation parameters



Conclusions

- At RT, a transition in the deformation mode occurs with grain size decreasing.
- Below at about 1 μm the deformation proceeds via SBs generation and widening
- The deformation within the SB is a complex interplay of lattice dislocations movement and grain boundary-related mechanisms (rotation, migration, sliding, damage...)
- At higher temperature, the *ufg* materials deform mostly via boundary mechanisms ($m \approx 0.5$); while the *mc* counterpart still deforms by lattice dislocations movement.

